1

Principles of Ultrasound Imaging and Signal Analysis

S. Lori BRIDAL
CNRS, INSERM, Laboratoire d'Imagerie Biomédicale (LIB),
Sorbonne Université, Paris, France

1.1. Introduction: probing living systems with ultrasound

A primary objective of medical imaging is to reveal something about a patient that cannot be evaluated by other means, while imposing as few constraints as possible on the operator and the patient during the imaging process. Ultrasound has many qualities relative to other imaging modalities that help it to contribute towards this goal. In addition to practical advantages such as portability and relative affordability, the nature of interactions between biological media and mechanical waves, and the speed of these interactions give ultrasound a unique place in the biomedical imaging armamentarium.

Within the power and amplitude ranges authorized for diagnostic ultrasound imaging, its innocuous nature has made it the method of choice for prenatal screening. Diagnostic ultrasound is also widely applied for cardiovascular imaging and to examine the liver, kidney, muscles, prostate, thyroid and superficial vessels. Spatial resolution can be adjusted within a range from about a millimeter to hundreds of micrometers, depending on the selected transducer and the explored depth. Images are constantly refreshed on the monitor in real time to provide a continuous sequence of images from the scanned regions. Conventional systems

For a color version of all the figures in this chapter, see www.iste.co.uk/bridal/innovative.zip.

Innovative Ultrasound Imaging Techniques,
coordinated by S. Lori BRIDAL.

offer imaging frame rates on the order of 50 images per second, and ultrafast systems can acquire data at frame rates reaching 20,000 images per second. Images are created from the sensitive detection of echoes returned from scattering structures of a tissue or organ and are presented on a grayscale where strongly reflecting interfaces or scattering structures are brighter. The resulting B-mode (brightness mode) images can be used to visualize the morphology of structures within the body – even those that are rapidly moving, like the beating heart. Doppler mode tracks the movement of red blood cells, and estimated values can be presented on a color scale overlaid on the morphological image to map out information about the blood flow speed, direction or concentration. Specially adapted ultrasound systems can deliver much higher acoustic intensity or power than that used for diagnostic imaging to a position that is selected by focusing. This can be applied, for example, to destroy a cancerous lesion or a kidney stone in zones that are difficult to reach with more conventional interventions.

This very versatile modality has a few notable limitations. Due to the relatively limited differences between the acoustic properties of soft biological tissues and the speckle pattern caused by the interference of echoes returned simultaneously to the transducer from sub-resolution-sized scattering structures, contrast between different types of tissues can be limited. This can hamper the detection of lesions or other anomalies. Compound imaging coherently adds echoes backscattered from the same imaged plane acquired from slightly different angles to reduce the effect of speckle. Image sequences are typically obtained in a single plane so that screening for anomalies relies on a sweep (most-often performed by hand) of the image plane through the volume of interest. Image placement and interpretation are very operator-dependent, so diagnosis can be influenced by the operator's choices and expertise. Growing capacities for three-dimensional ultrasound alleviate these limitations to some degree but, for full-body screening, ultrasound is still outranked by techniques like positron emission or X-ray tomography. Key ultrasound imaging advantages and limitations are summarized in Figure 1.1. Research is underway to curtail limitations and further empower ultrasound's ability to probe living systems.

Consider a typical ultrasound image (see Figure 1.2). The source of ultrasound, the ultrasonic probe, is positioned against the body (at the top of the image in Figure 1.2), and the cross-section of the body in the line of sight of the probe is mapped out in grayscale beyond this surface. Echoes from zones farther from the probe return to the probe later than echoes from more superficial regions so that, along the propagation axis, the echo time delay describing the lapse of time between the emission of the ultrasound pulse and echo reception, Δt_{echo}, is related to the

average speed of sound propagation in the medium, c, and the depth, D, of the echogenic structure simply by relating the round-trip travel time to the depth:

$$2D = c \cdot \Delta t_{echo} \quad [1.1]$$

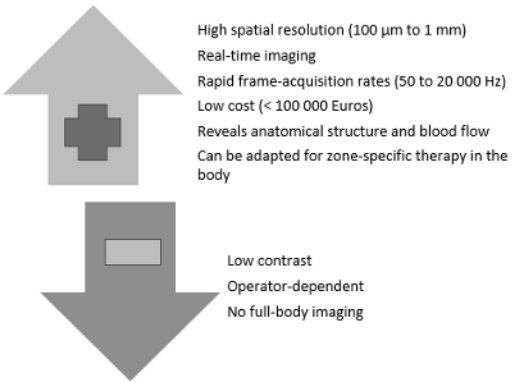

Figure 1.1. *Key advantages and limitations of ultrasound*

The on-screen display identifies the type of ultrasound probe used to make the image (ultrasonic frequency and other salient characteristics). The mechanical index and thermal index can also be displayed to show that imaging safety limits have been respected and that the system is operating under conditions that will not create either cavitation or significant heating in the body. The number of images recorded per unit time, which is referred to as the frame rate, is typically presented in units of Hz or frames per second (fps). If we look more closely at the image, we may note that there are some bright and well-defined boundaries where the ultrasound wave has been reflected from surfaces between different types of tissues or organs. Zones in between such clear boundaries present a speckled brightness pattern instead of a uniform level of gray. Also, deeper regions can present a lower, average brightness than the more superficial regions of the same organ because the ultrasonic wave reaching these deeper zones and the echoes returned from them are more strongly attenuated.

This first chapter will present the basic concepts behind the formation of ultrasound images and, for each key aspect of ultrasound imaging, the subsequent chapters will provide deeper insight into specific ultrasonic techniques and a look at the most promising current innovations that are moving these techniques forward towards the next generation of ultrasound imaging.

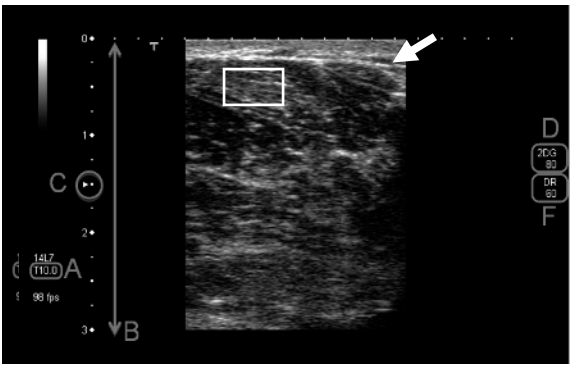

Figure 1.2. *Ultrasound B-mode image with an on-screen display of probe and imaging settings. In this case, the probe is a linear array transducer with a frequency range from 7 to 14 MHz (probe label, 14L7). The selected central transmit frequency in MHz (A), imaging depth in cm (B), focal position marked by arrowheads (C), gain in dB (D) and display dynamic range in dB (F) are shown on-screen. The white arrow designates a bright echo from a boundary, and the white box outlines a zone of speckle pattern. No decrease in the average brightness of the speckle pattern with depth is apparent in this image because time gain compensation (gain that increases as a function of depth) has been applied*

1.2. Ultrasound probes

1.2.1. *Piezoelectric materials: electro-acoustic conversion*

Creating and detecting ultrasonic signals relies on the use of piezoelectric (PZT) materials. In 1880, Pierre and Jacques Curie discovered that applying a mechanical constraint along a selected axis of certain types of crystals led to the creation of an electrical potential across the crystal ("Piezo" comes from a Greek word for pressure). PZT materials are dielectric, which means that they are poor conductors of electric current. Thus, if the specifically arranged, electrical charges associated with the atoms within them are displaced minutely, a global charge distribution is created such that the crystal presents a net charge or electrical potential across its opposite faces. This is known as the direct piezoelectric effect (see Figure 1.3(a)). It works the other way too. The negative charges within the PZT material shift by a tiny amount to counter-act an electric field applied across the material, and this induces a tiny global deformation of the material's thickness in response to an applied electric potential. This is known as the inverse piezoelectric effect (see Figure 1.3(b)). By alternating positive and negative electric potentials across the crystal, the PZT can be made to mechanically vibrate. PZT materials provide the means for the electro-acoustic conversion used to generate and receive ultrasound signals.

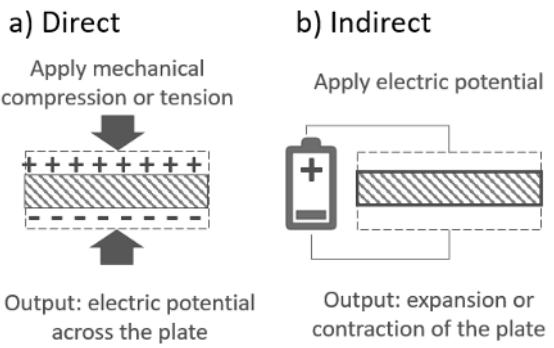

Figure 1.3. *Direct and indirect (or inverse) piezoelectric effects are used for electro-acoustic conversion*

1.2.2. *Transducers*

The handheld ultrasonic probe generally contains an assemblage of PZT elements within its tip that are arranged geometrically to best adapt to the desired scanning conditions needed for the organ or zone to be examined. This ultrasonic transducer array of PZT elements converts electrical energy into acoustic energy and vice versa. For linear transducer arrays, the PZT elements are aligned in a row and the transducer will produce a rectangular set of scan lines. In a convex array, the PZT elements are arranged in a curvilinear fashion (along the arch of a curve) so that the scan lines can fan out from the ultrasound source to evaluate a zone that widens with depth. This can be very useful for the evaluation of large organs at greater depths within the body or for situations where there is only a limited space on the body's surface through which to transmit sound. A position on the body where the transducer can be placed to provide a pathway for wave propagation within the body without the obstruction of the transmitted signals is known as an acoustic window. For example, for cardiac imaging, the transducer has to be placed in the limited space between the ribs to achieve effective ultrasonic transmission. Matrix arrays have PZT elements arranged across a rectangular, 2D grid so that 3D imaging of full volumes can be performed. Other arrangements may be designed to image from within cavities or for specialized applications. Diagrams of some of the possible element arrangements are shown in the next chapter in Figure 2.3.

Each PZT element is electrically connected by depositing a thin layer of conductive material on its surfaces so that there is a positive electrode on the back of

the element and a ground electrode on the front. Electrical impedance matching is necessary to optimize the electromechanical coupling between the system electronics and the PZT element. The rear side of each PZT element is adhered to a backing. For imaging, the backing properties are designed to absorb ultrasound propagating within the housing of the transducer. This backing is also important for damping the resonance of the transducer so that the length of transmitted pulses can be limited in time (shorter pulse duration, higher bandwidth). The face plate of the ultrasound probe is designed to optimize the transmission of ultrasound from the PZT elements of the transducer into the body. To do this, quarter wavelength matching layers with an acoustic impedance, Z_{match}, between that of the transducer material, Z_{PZT}, and that of the body's superficial tissue, Z_{body}, are embedded in this interface ($Z_{match} = \sqrt{Z_{PZT} \times Z_{body}}$). Finally, an acoustic coupling gel is used to prevent air-spaces between the ultrasonic probe and the patient, because even a thin layer of air will interfere strongly with the effective transmission of ultrasound.

The characteristic acoustic impedance of a material, denoted as Z, has a definition analogous to Ohm's law (voltage = impedance times current) that relates the acoustic impedance to the local particle displacement, $\dot{u} = \frac{du}{dt}$, and pressure, p, produced by a propagating acoustic wave:

$$Z = \frac{p}{\dot{u}} \qquad [1.2]$$

Since the pressure at a specific point caused by an acoustic wave is related to the material's density, ρ, the wave's speed, c, and the particle displacement as described by:

$$p = \rho \cdot c \cdot \dot{u} \qquad [1.3]$$

the characteristic acoustic impedance can also be expressed in terms of the density and the speed of sound in the medium of propagation, which is the PZT material in this case:

$$Z = \rho \times c. \qquad [1.4]$$

1.2.3. *Modeling the transducer response*

The transducer crystal can vibrate resonantly after excitation with a brief impulsion, or it can be forced to vibrate at a selected driving frequency. The level of damping will determine the system's tendency to resist oscillation and the rate of decay of mechanical oscillations after the application of an electrical impulsion

across the crystal's electrodes. This behavior is reminiscent of the familiar response of a damped harmonic oscillator (see Figure 1.4(a)), for which Hooke's law relates the force, F_S, on a mass attached to a spring with a positive spring constant, k [N m^{-1}], to the displacement of the mass, x, relative to its initial equilibrium position at $x = 0$:

$$F_S = -k \cdot |x| \qquad [1.5]$$

Such a system will oscillate at some natural resonance frequency after excitation with an impulsion. It can also be driven to oscillate with a time-varying force $F(t) = a \sin \omega t + b \cos \omega t$, where a and b are constants and ω is the angular frequency of the applied oscillations. As illustrated in Figure 1.4, the oscillations produced by the applied force are subject to mechanical damping.

Damped harmonic oscillator systems can be simulated with an equivalent circuit model. To build intuition about this kind of model, consider the very simple RLC circuit where a time-varying voltage produces a current, *i(t)*, in a circuit composed of a capacitor, a resistor and an inductor in series (see Figure 1.4(b)). In the circuit, energy is stored in an electric field across the capacitor. The inverse of electrical capacitance, *1/C*, is analogous to the spring constant, *k,* of the mass–spring system. Energy can also be charged in the magnetic field as current flows through the inductor. The electric inductance, *L*, is analogous to the mass on the spring (or the equivalent mass of a transducer system). The energy is dissipated by the electrical resistance, *R*, which is analogous to mechanical damping. Finally, the applied electrical potential, *V(t)*, in the circuit is analogous to the applied mechanical force, *F(t)*, used to drive the mass–spring system. The oscillating mass–spring, the transducer and the circuit all exhibit resonant behavior. For the circuit, this resonance can be varied by changing the values or the arrangement of R, L, C components.

Equivalent circuit models can be used to simulate the properties (frequency bandwidth, sensitivity, driven and natural resonant frequencies, etc.) that will be obtained for a specific transducer design (choice of piezoelectric material, thickness, acoustic and electrical matching). The model is based on parallel and series RLC components (resistors, capacitors and inductors) that represent transducer properties, such as the mechanical damping, the mass, elastic compliance and electrostatic capacitance between the faces of the PZT element. Two classic equivalent circuit models for transducers, and the characteristics that they can be used to evaluate, are explained in more detail in Chapter 2.

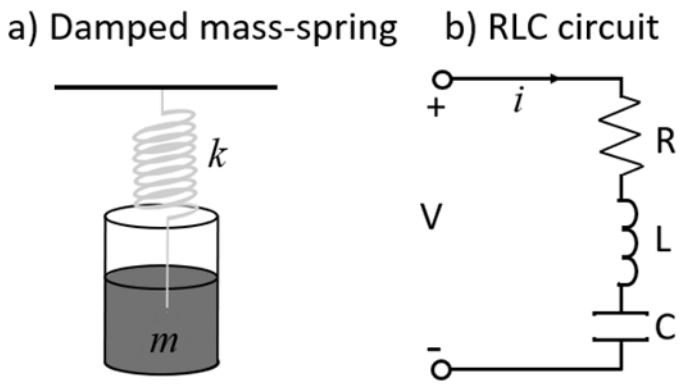

Figure 1.4. *Damped harmonic oscillators: a) spring and mass in oil, b) RLC circuit*

1.2.4. *Frequency and period of oscillation*

In the mass–spring and RLC circuit analogies, the driving force can be a sinusoidally oscillating force at an angular frequency of ω. The frequency, f, measured in Hz (hertz) designates the number of oscillatory cycles per second (e.g. if the spring is vibrating at 1 Hz, the movement will complete a full cycle from the lowest position of the mass to the highest position of the mass and back again to the lowest position in one second). The angular frequency, ω, describes an angular displacement per unit time in units of radians per second. The two quantities are related by a simple equation:

$$\omega = 2\pi f = \frac{2\pi}{\tau} \qquad [1.6]$$

As the mass moves through the different stages of its oscillation, the angular frequency describes the rate of change of the phase as a function of time of the sinusoidal waveform that would map out the amplitude of the displacement of the mass relative to its equilibrium position, as illustrated in Figure 1.5. The period of oscillation, τ, describes how long it takes for a complete cycle of oscillation and is the inverse of the frequency of the oscillation:

$$\tau = \frac{1}{f} \qquad [1.7]$$

By describing the fractional number of oscillatory periods that have occurred at time, t, as $\frac{t}{\tau}$, the displacement of the mass as a function of time can be written using

a sinusoidal function, where the position of the oscillating mass relative to the equilibrium position at $x = 0$ at any time, t, is:

$$x(t) = x_{max}\, sin\left(2\pi\frac{t}{\tau}\right) = x_{max}\, sin\,(\omega \cdot t). \quad [1.8]$$

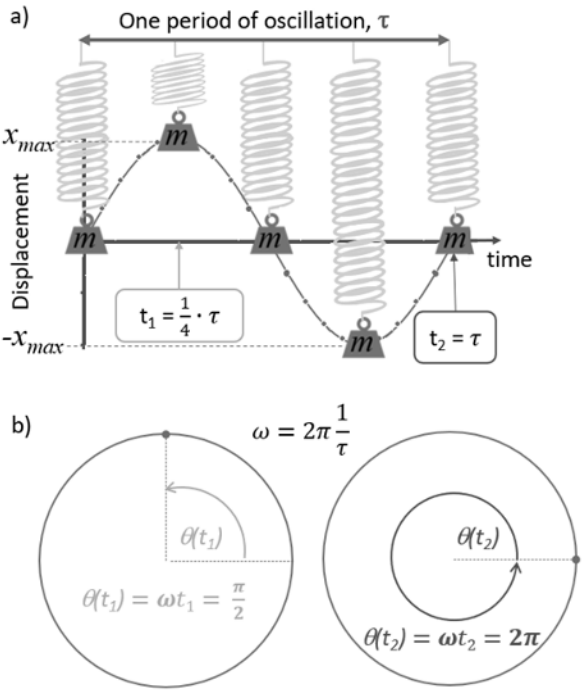

Figure 1.5. *Relating linear and angular frequency. a) As the mass oscillates about its equilibrium position, the linear frequency of oscillation, f, is the number of cycles per second, which is the inverse of the period of oscillation, τ. b) Angular frequency, ω, in units of radians per second can be used to express the cyclical nature of the motion. A period of oscillation is completed after each full rotation of 2π*

1.2.5. *Transducer resonant frequency and bandwidth*

For ultrasonic transducers, the thickness of the PZT elements is tailored to respond optimally at a selected resonant frequency, $f_{PZT\,Res}$. If we excite a piezoelectric plate of thickness, **t**, with an electrical impulse, the plate will have a natural, thickness-mode resonance frequency when the round-trip distance of

vibration $2t$ is equal to the speed of sound in the material, c_{PZT}, times the time required for one cycle of vibration (one period) τ:

$$2t = c_{PZT}\tau \text{ so that } f_{PZT\,Res} = \frac{c_{PZT}}{2t} \quad [1.9]$$

A thicker crystal has a lower thickness-mode resonance frequency, and a thinner crystal resonates at a higher frequency. For the PZT elements used for biomedical ultrasound, this frequency is typically in the MHz range for excitation with an electrical impulse or gated excitation voltage, and the longitudinal mechanical wave created by the oscillation is in the ultrasonic range – at frequencies much too high to be heard with the human ear.

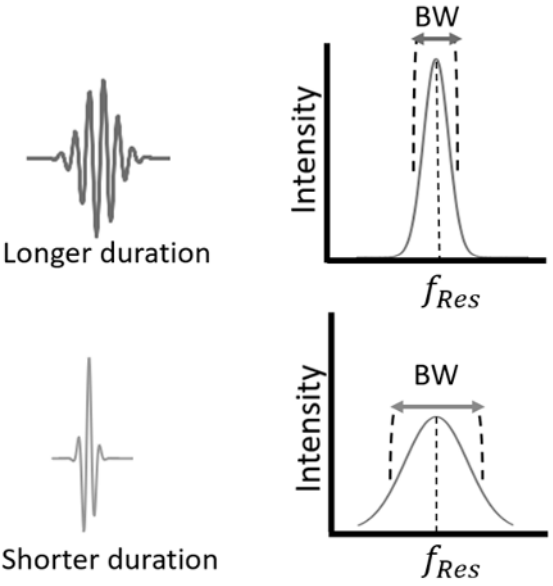

Figure 1.6. *At a fixed frequency, the less highly damped pulse has a longer duration in time and a narrower bandwidth, BW, in the frequency domain than a more highly damped one*

An ultrasound pulse created with a piezoelectric plate of thickness **t** will, in general, contain a range of frequencies with peak energy at the thickness-mode resonance frequency, $f_{PZT\,Res}$, of the PZT plate. By taking the Fourier transform of the pulse, the amplitude of the energy in the pulse can be represented in the frequency domain based on its weighted frequency content, as shown in Figure 1.6. The range of the significant frequency response included in the transmitted pulse is

referred to as the bandwidth. It is inversely related to the pulse duration, which is influenced by the frequency of the transducer and its damping. The bandwidth can be defined as the range of frequencies within which the intensity is greater than or equal to -3 dB of the peak spectral amplitude. If the pulse has not been detected directly, but rather evaluated based on the reflection from a perfect reflector, the same bandwidth can be identified by searching for the range of frequencies within -6 dB of the peak of the Fourier transform of the reflected pulse (50% of the spectrum's peak amplitude). The more strongly damped the PZT plate, the shorter the pulse and the wider the bandwidth, but the pulse also contains less energy when it is strongly damped.

1.3. Longitudinal ultrasound waves

1.3.1. *Vibrations along the axis of wave propagation*

A pulse generator emits an electric pulse that is used to excite the PZT elements in the ultrasound transducer so that the energy in the electrical pulse is converted to a mechanical vibration that is coupled into the body as a mechanical wave. Ultrasound propagates into the body in the form of a longitudinal, compressional wave. Thus, as the energy of the wave is transmitted from the transducer into the medium and moves through the medium where ρ_0 and p_0 are, respectively, the ambient density and pressure in the medium, the molecules are displaced slightly from their equilibrium positions along the axis parallel to the propagation of the wave to temporarily form zones of compression (molecules are closer together than usual so the material is effectively denser $\rho = \rho_0 + \Delta\rho$, $\Delta\rho > 0$ and the local pressure is increased, $p = p_0 + \Delta p$, $\Delta p > 0$) alternating with zones of rarefaction (molecules are farther apart than usual so the material is effectively less dense $\rho = \rho_0 + \Delta\rho$, $\Delta\rho < 0$ and the local pressure is decreased, $p = p_0 + \Delta p$, $\Delta p < 0$). The local particle displacement leads to a modification of the local pressure and the local density as the medium is compressed or rarefied. This is diagrammed in Figure 1.7 for a continuous wave. The distance labeled with the symbol λ in the figure corresponds to the acoustic wavelength, the distance between positions where the particle displacement is at the same point in the cyclic motion or, stated differently, the distance between two points of matched phase and amplitude. In this illustrated case, the wavelength is shown between two zones of maximum compression. It should be kept in mind that zones of maximum rarefaction, maximum compression and all the relative levels of compression and rarefaction in between can be considered to have an approximately homogeneous local pressure and density on a scale $<< \lambda$.

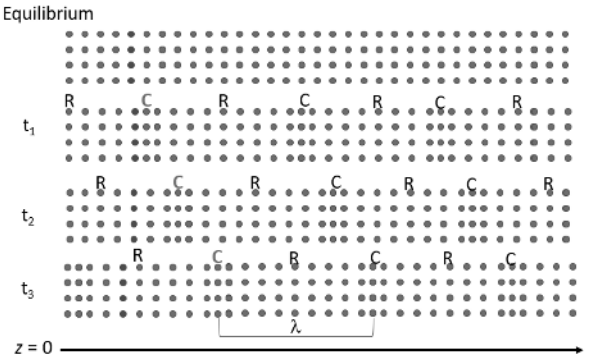

Figure 1.7. *The molecules or particles of a material, represented by the blue disks, at equilibrium (top row). Imagine that a transducer placed flush against the particles at z = 0 is creating a continuous vibration that propagates along the z axis. Zones of compression, C, and rarefaction, R, are formed in the propagation medium. Each compressive and rarefactive disturbance propagates steadily to deeper positions in the material as a function of time, t. A set of particles is labeled with red disks to illustrate that the particles vibrate about their fixed equilibrium position as the wave's energy propagates in z*

1.3.2. *The 1D, elastic wave equation*

Ultrasonic waves are mechanical waves that result from the transfer of energy in the form of a traveling disturbance in the density and pressure of the propagation medium. The wave propagates as this disturbance moves away from the source. Hooke's law, Newton's second law of motion and the continuous medium theorem are used to express this disturbance in the form of the wave equation. If we consider infinite plane waves in a lossless elastic medium, the propagation of this local disturbance in the density and pressure within the propagation medium can be considered in one dimension for simplicity. Consider the 1D propagation medium as a row of atoms or particles where each has mass, m, and they are elastically coupled to one another by springs where each spring has the same elastic constant, k. Unperturbed by a sound wave, the particles are equally separated by a distance a. The elastic force on particle n exerted by its two neighbors is:

$$F^{eq.}_{(n-1)\to n} = k\{(n-1)\cdot a - n\cdot a\} = -ka \quad [1.10]$$

$$F^{eq.}_{(n+1)\to n} = k\{(n+1)\cdot a - n\cdot a\} = ka \quad [1.11]$$

The net force on particle n at equilibrium is therefore the sum of equations [1.10] and [1.11] such that:

$$F^{eq.}_{(n-1)\to n} + F^{eq.}_{(n+1)\to n} = -ka + ka = 0. \quad [1.12]$$

If the first particle in this chain is moved slightly away from its equilibrium position by some force (our vibrating ultrasound transducer), its displacement will exert a force on its neighbor via the connecting spring, and a series of displacements will be transferred from one particle to the next to propagate farther and farther along the chain of particles (see Figure 1.8). Once the disturbance has passed by a region, the restoring force of the springs between the particles will return them to their equilibrium positions.

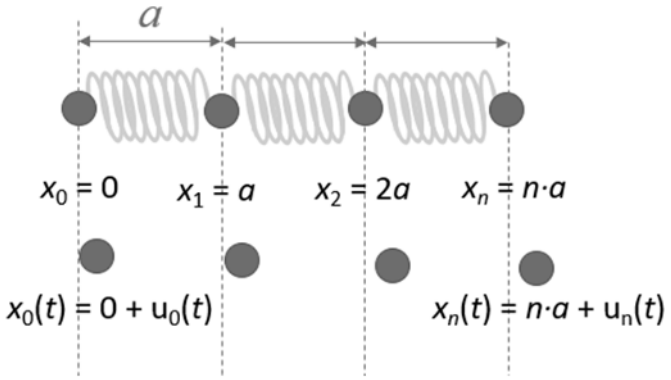

Figure 1.8. *Each particle is initially at a position $x_n = n{\cdot}a$. When displaced from equilibrium, the perturbed position for each can be written as $x_n = n{\cdot}a + u_n(t)$, where $u_n(t)$ is the displacement at time t relative to the particle's equilibrium position*

Since the forces between particles at equilibrium cancel each other out, the net force will only depend on the relative extension or compression of the "springs" between a particle and each of its neighbors. The additional force imposed by particle n-1 on particle n is thus:

$$F_{(n-1)\to n}(t) = k\big(u_{n-1}(t) - u_n(t)\big) \quad [1.13]$$

The additional force due to the displacement of particle n+1 on particle n is:

$$F_{(n+1)\to n}(t) = k\big(u_{n+1}(t) - u_n(t)\big) \quad [1.14]$$

So, the overall force on particle *n* as a function of time is:

$$F_{(n-1)\to n}(t) + F_{(n+1)\to n}(t) = k\big(u_{n-1}(t) - u_n(t)\big) + k\big(u_{n+1}(t) - u_n(t)\big)$$

$$= -k\big(2 \cdot u_n(t) - u_{n-1}(t) - u_{n+1}(t)\big) \quad [1.15]$$

Since the relative displacements that occur at the particles *n*-1, *n* and *n*+1 in the medium occur on the scale of the spacing between atoms in matter (a scale of Angstroms or 10^{-10} meters), and since transducers create vibrations in biological media with characteristic lengths on the order of hundreds of millimeters or micrometers (> 10^{-4} meters), there should only be a very small difference in the relative displacements between atoms *n*-1, *n* and *n*+1. The medium can therefore be considered as a continuum where the displacement can be characterized for every position *x* as *u*(*x*, *t*) and a second-order Taylor expansion can be applied to estimate the displacements at the positions $x_{n-1} = x_n - a$ and $x_{n+1} = x_n + a$:

$$u_{n-1}(t) \to u(x_{n-1}, t) \cong u(x_n, t) - \frac{\delta u}{\delta x} a + \frac{1}{2}\frac{\delta^2 u}{\delta x^2} a^2 \quad [1.16]$$

$$u_{n+1}(t) \to u(x_{n+1}, t) \cong u(x_n, t) + \frac{\delta u}{\delta x} a + \frac{1}{2}\frac{\delta^2 u}{\delta x^2} a^2 \quad [1.17]$$

Partial derivatives are used since the displacement depends on both time, *t*, and position, *x*. Using equations [1.16] and [1.17], equation [1.15] becomes:

$$F_{(n-1)\to n}(t) + F_{(n+1)\to n}(t) = -k\big(2 \cdot u(x_n, t) - u(x_{n-1}, t) - u(x_{n+1}, t)\big)$$

$$= -k\left(2 \cdot u(x_n, t) - \left[u(x_n, t) - \frac{\delta u}{\delta x} a + \frac{1}{2}\frac{\delta^2 u}{\delta x^2} a^2\right] - \left[u(x_n, t) + \frac{\delta u}{\delta x} a + \frac{1}{2}\frac{\delta^2 u}{\delta x^2} a^2\right]\right)$$

$$= k \cdot \frac{\delta^2 u}{\delta x^2} a^2 \quad [1.18]$$

From Newton's second law of motion, the force on a moving object equals its mass times its acceleration. The elastic force described above can thus be related to the acceleration of the particle motion to obtain the one-dimensional wave equation for a wave in an elastic medium

$$m\frac{\delta^2 u}{\delta t^2} = k \cdot \frac{\delta^2 u}{\delta x^2} a^2$$

$$\frac{\delta^2 u}{\delta x^2} - \frac{m}{a^2 k}\frac{\delta^2 u}{\delta t^2} = 0 \qquad [1.19]$$

Consider now a block of material. Hooke's law for a bar of material states that the force, $F_\perp$, per unit area, S, applied perpendicularly to the surface of the material is equal to Young's modulus, E, times the relative deformation of the material along its length, l:

$$\frac{F_\perp}{S} = E \cdot \frac{\Delta \iota}{\iota} \qquad [1.20]$$

For the chain of particles, Hooke's relation is expressed as:

$$F_\perp = k \cdot (u_{n+1} - u_n) \qquad [1.21]$$

Consider that the surface area, S, of the face of a material can be divided into tiny squares of surface area, a^2, where each of these squares contains one of the particle chains. The force due to a tiny displacement of this surface will be multiplied by the number of chains of particles that are being disturbed $n = S/a^2$. For the application of a force to a surface area of material, therefore, the equation above, expressed in terms of the elastic constant between individual particles, k, is:

$$F_\perp = \frac{S}{a^2} k \cdot (u_{n+1} - u_n) \qquad [1.22]$$

$$\frac{F_\perp}{S} \cong \frac{k}{a^2} \cdot \left(\frac{\delta u}{\delta x} a\right) \cong \frac{k}{a} \cdot \left(\frac{\delta u}{\delta x}\right) \qquad [1.23]$$

It is practical to rewrite the wave equation in equation [1.19] using the relations $E \cong k/a$ and $\rho = m/a^3$ to refer to quantities that characterize material properties for the continuous medium:

$$\frac{\delta^2 u}{\delta x^2} - \frac{ma}{a^3 k}\frac{\delta^2 u}{\delta t^2} = 0 \qquad [1.24]$$

$$\frac{\delta^2 u}{\delta x^2} - \frac{\rho}{E}\frac{\delta^2 u}{\delta t^2} = 0 \qquad [1.25]$$

1.3.3. *The propagating wave*

The development in the previous section was made considering that the displacement could be described by a plane wave. Its general solution is:

$$u(x, t) = f_1(t+x/c) + f_2(t-x/c) \qquad [1.26]$$

where f_1 describes a propagation towards negative x and f_2 describes a propagation towards positive x (at a speed of c). Taking the partial derivatives of this solution that are found in the wave equation (equation [1.25]):

$$\frac{\delta^2 u}{\delta t^2} = u(x,t) \quad [1.27]$$

$$\frac{\delta^2 u}{\delta x^2} = \frac{1}{c^2} u(x,t) \quad [1.28]$$

and putting equations [1.27] and [1.28] into the wave equation [1.25], the following is obtained:

$$\frac{1}{c^2} u(x,t) - \frac{\rho}{E} u(x,t) = 0 \quad [1.29]$$

$c = \sqrt{\frac{E}{\rho}} = \sqrt{\frac{1}{\rho k}}$, where κ is the compressibility of the medium that relates the change in pressure to the change in density, $\kappa = \frac{dp}{d\rho}$. Thus, the speed of sound, c, in the medium is related to the density and compressibility of the medium. A more rigid material with low compressibility will typically exhibit a higher longitudinal speed of sound than a less rigid (more compressible) material.

The particle displacement shown in Figure 1.7 can be presented in terms of density, pressure or particle displacement at a given position as a function of time, as shown in Figure 1.9. At any selected position in the medium, the time it takes for the vibration to complete a full cycle is the period of the wave, τ. The frequency is the number of cycles per unit time so that the frequency is related to the period according to $\tau = \frac{1}{f}$. Since the period is the time for one full cycle of vibration to occur and since the wave is traveling at a speed of c, the wavelength (distance between two points of matched phase and amplitude) can be expressed in terms of the speed of the wave propagation times the wave period $\lambda = c \cdot \tau$, or as the speed of wave propagation divided by the wave frequency: $\lambda = \frac{c}{f}$. As a function of time, the perturbation repeats itself every period. As a function of position, the perturbation pattern is repeated every wavelength.

A sine wave is a simple solution to the wave equation. For a continuous waveform advancing towards positive x, the pressure can thus be described by a sinusoidal function so that $p(x,t) = p_{max}\, sin\left(2\pi\left[\frac{t}{\tau} - \frac{x}{\lambda}\right]\right) = p_{max}\, sin\left(\omega\left[t - \frac{x}{c}\right]\right)$.

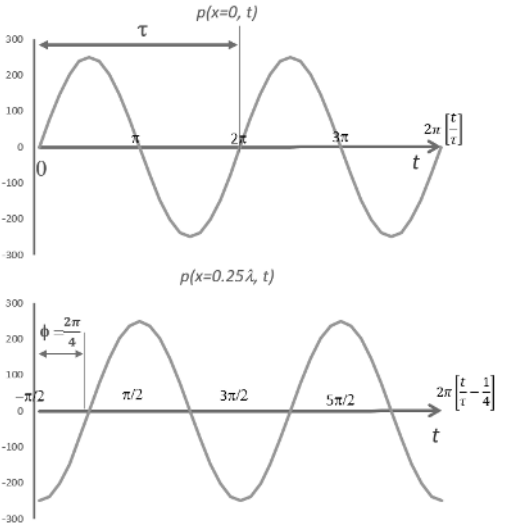

Figure 1.9. *At a fixed position x in the medium, the pressure, p, as a function of time for a continuous wave is described by* $p(x,t) = p_{max}\, sin\left(2\pi\left[\frac{t}{\tau} - \frac{x}{\lambda}\right]\right)$. *At other positions in the medium (e.g. x = 0.25λ in the bottom graph), the pressure presents the same periodicity, but is offset in time by a phase φ = 2π(x/λ)*

1.4. Pulse-echo ultrasound

1.4.1. *Ultrasonic pulses*

For imaging, pulses of ultrasonic waves are transmitted into the medium instead of continuous waves. The pulse generator emits a brief electrical pulse to excite the transducer. That brief change in electrical potential is converted to an ultrasound pulse through the inverse piezoelectric effect. Pulses can be represented as Gaussian-modulated sinusoidal waves (a gated portion of an oscillating wave):

$$p(x,t) = p_{max} e^{\frac{-\sigma^2\left[t-\frac{x}{c}\right]^2}{2}} sin\left(\omega\left[t - \frac{x}{c}\right]\right) \qquad [1.30]$$

Such pulses will be sent repeatedly at a rate that is consistent with the time needed to explore the full depth of the region:

$$2 \times [Maximum\ depth\ to\ explore] \leq c \times [time\ between\ two\ pulses] \qquad [1.31]$$

The pulse duration, *PD*, is the time between the "beginning" and the "end" of the ultrasound pulse. A specific level can be chosen in dB (e.g. -20 dB) to precisely establish what amplitude levels relative to the peak amplitude correspond to the effective beginning and end of the envelope of the pulse. The *PD* is illustrated relative to the pulse repetition interval, T_{PRI}, in Figure 1.10. The pulse duration is typically on the order of a few periods of acoustic oscillation ($PD = [\#\ cycles] \times \tau$ is on the order of a few microseconds for MHz range ultrasound) so that the pulse contains only a small number of wavelengths. The pulse repetition interval is much longer (hundreds of microseconds to milliseconds) so that each pulse can complete the round-trip time to and back from the deepest region to explore before the next pulse is initiated.

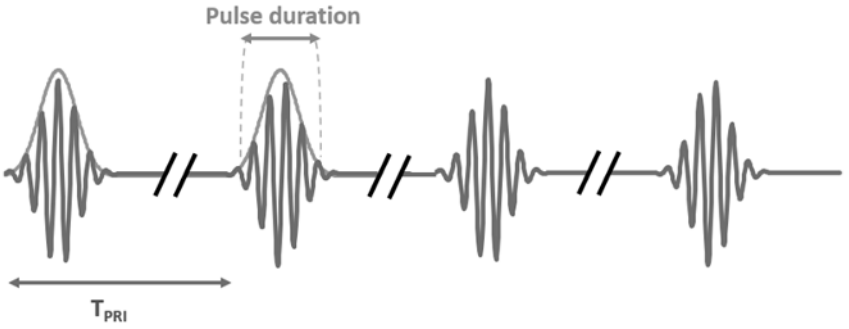

Figure 1.10. *Gaussian-modulated pulse repeated at a pulse repetition interval of T_{PRI}. The black break points show that the time scale is not continuous between pulses because the pulse repetition interval is much longer than the pulse duration. The pulse repetition frequency is the inverse of the pulse repetition interval*

1.4.2. *Pressure and intensity*

The pressures used for ultrasonic imaging are limited, as described with respect to the mechanical index (equation [1.41]). Thus, depending on the frequency, pulse pressures are in the 100 kPa to a few MPa pressure range. This can be compared to the equilibrium or atmospheric pressure, which is 100 kPa. Therapeutic ultrasound can use much higher pressures in the megaPascal range.

Intensity is defined as power per unit area. For a continuous acoustic wave creating cyclical changes in the pressure and the particle displacement of a medium, the average power transported per unit area is:

$$\hat{I} = \frac{1}{\tau}\int_0^{\tau} p\,(t) \times u\,(t)\dot{dt} = \frac{1}{2} p_{max} \cdot \dot{u}_{max} \qquad [1.32]$$

When considering the intensity for pulsed ultrasound, the temporal-averaged intensity is found based on the average intensity during an individual pulse multiplied by the active fraction of the duty cycle, where the duty cycle is the pulse duration divided by the pulse repetition interval:

$$Temporal - average\ intensity = Avg.pulse\ intensity \times \frac{PD}{T_{PRI}} \qquad [1.33]$$

The geometrical distribution of the energy in the ultrasound beam can also be considered. There are regulatory limits on the spatial average temporal average (SATA) and other associated parameters used to characterize the acoustic intensity delivered during imaging.

1.4.3. *Central frequency choice*

The central frequency of the ultrasonic pulse can be adapted to the application. For a fixed level of damping, the pulse length can be essentially limited to a fixed number of wavelengths. Since high-frequency transducers create shorter wavelengths, they can provide shorter pulses and improved axial resolution. Higher frequencies can provide a better spatial resolution, but they are also more strongly attenuated in biological media. To image the abdominal organs or the heart, frequencies near 2 MHz are generally used. Imaging of more superficial regions, such as the breast, can call upon higher frequency transducers (approximately 10 MHz). To examine structures in the eye or to image small animals, the frequencies can be further increased to more than 20 MHz. For therapy, frequencies near 1 MHz are often chosen.

1.4.4. *Attenuation*

The attenuation, generally expressed in dB per cm, describes the exponential loss of signal as a function of the total propagation distance through an attenuating medium that is due to both scattering and absorption processes. This limits the depth that can be effectively imaged. To estimate the signal loss due to attenuation, it is

important to apply the coefficient appropriately for the relative loss of amplitude or intensity:

$$Pressure\ amplitude\ (z) = p_{max}(z=0)e^{-\left(\frac{Attenuation\ in\ dB/cm}{8.686}\cdot z\right)} \quad [1.34]$$

$$Intensity\ (z) = I_{max}(z=0)e^{-\left(\frac{Attenuation\ in\ dB/cm}{4.343}\cdot z\right)} \quad [1.35]$$

The attenuation of ultrasonic signals in biological media is stronger for higher frequencies (shorter wavelengths) so the signal-to-noise ratio decreases more rapidly with depth for higher frequencies. In most biological materials within the range of frequencies used for diagnostic imaging, the attenuation can be expressed as a factor of proportionality in dB/cm-MHz. Thus, for a given medium, the number of decibels lost per cm of propagation distance is twice as high at 10 MHz as compared to 5 MHz. Attenuation also depends on the type of media encountered along the propagation path. Ultrasound loses relatively little of its energy as it progresses through water: about 0.01 dB/cm at 5 MHz. Tissues like breast or liver attenuate about 3 dB/cm for an ultrasonic wave at 5 MHz. Lungs and bones attenuate very strongly (tens of dB/cm at 5 MHz) so that it becomes very difficult to transmit ultrasound through these materials.

1.4.5. *Propagation speed*

Within most soft tissues in the body, sound propagates at a speed of approximately 1,540 m/s. There are subtle differences, however, between the speed of propagation in different types of biological tissues. Transmission through layered soft tissues can degrade images due to an effect called phase aberration. For example, the speed of sound in a layer of fat is slightly lower than that in more muscular tissue so that waves propagating through different thicknesses of fat will present slight phase offsets with respect to each other. Phase aberration and methods to correct it are described in Chapter 8. The speed of sound can also be modified by anisotropic properties within the medium. For example, within muscles, the fibers can be arranged in a regular arrangement about a specific axis. This is particularly true within the Achilles tendon. Ultrasound will propagate significantly faster along the direction aligned with muscle or tendon fibers than along the direction perpendicular to the fiber orientation.

1.4.6. *Nonlinear propagation effects*

As shown in Figure 1.7, the wave itself modifies the local pressure (and density) in the medium it is propagating through. The zones that are denser have faster sound

speed than zones at lower density. In general, this effect is negligible, but if the relative change in pressure/density produced by the wave is strong or if the wave is propagating across a large distance, the wave can become distorted due to this nonlinear effect. The higher the pressure amplitudes in the wave, the more quickly nonlinear components will accumulate. More highly compressible propagation media (like fatty tissue) are also prone to enhancing nonlinear propagation.

During nonlinear wave propagation, the frequency content of the wave will be modified so that high-frequency components accumulate. This will change (increase) the attenuation of the wave and also lead to harmonic content. The shift in the spectral content due to higher frequency, nonlinear tissue harmonics can be used to improve the resolution (tissue-harmonic imaging) of finer details and improve imaging from deeper regions.

1.4.7. *Reflection, transmission and refraction*

As for transducer materials, biological materials also have an acoustic impedance that is related to the density of the material multiplied by its speed of sound. At a smooth interface with dimensions >> λ that is between two media with different characteristic impedances, Z_1 and Z_2, a fraction of the intensity in an ultrasonic plane wave will be reflected back towards the transducer, while the rest will be transmitted across the interface and continue propagating away from the transducer, as diagrammed in Figure 1.11. If the interface is perpendicular to the direction of wave propagation, the fraction of the reflected intensity is:

$$R_I = \frac{(Z_2 - Z_1)^2}{(Z_2 + Z_1)^2} \quad [1.36]$$

And the remaining fraction is transmitted:

$$T_I = 1 - R_I \quad [1.37]$$

Very strong reflections occur at interfaces between tissues and gas-filled regions of the body (gas-filled bowel, for example). A much smaller part of the intensity, typically less than 0.1%, is reflected from boundaries between soft tissues.

If the interface is not perpendicular to the direction of wave propagation so that the incident wave arrives at an angle of θ_i with respect to the interface, the reflected

wave will be reflected and the transmitted signal will be refracted at an angle determined by the relative speeds of sound in the two materials:

$$\theta_t = \left[\frac{c_2}{c_1} sin\ \theta_i\right] \quad [1.38]$$

where c_1 and c_2 represent the speed of sound in the first and second tissues encountered. Thus, the greater the difference in the speed of sound between the two media, the more strongly the transmitted sound will be refracted or deviated from its original path. In this case, the fraction of reflected intensity can be expressed as:

$$R_I = \frac{(Z_2 cos\ \theta_i - Z_1 cos\ \theta_t)^2}{(Z_2 cos\ \theta_i + Z_1 cos\ \theta_t)^2} \quad [1.39]$$

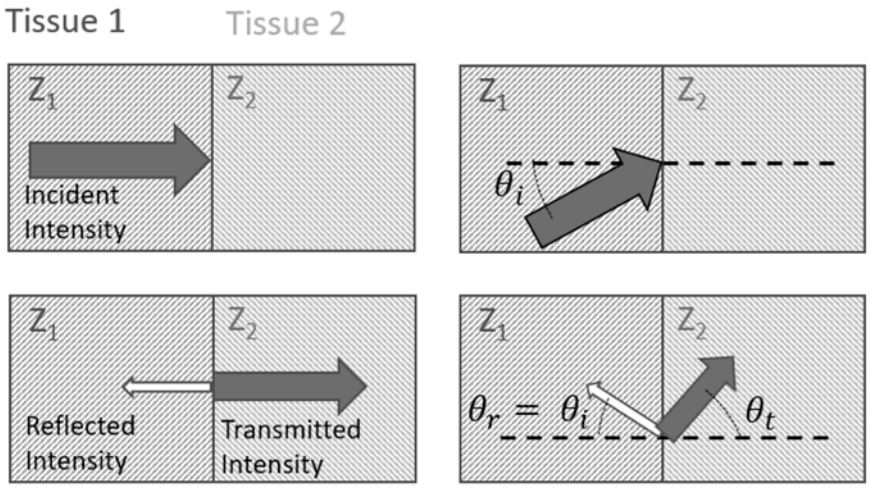

Figure 1.11. *Intensity of the energy in an ultrasonic plane wave incident upon a smooth interface with dimensions much greater than that of the ultrasound wavelength will be partially reflected and partially transmitted according to equations [1.36] and [1.37] for perpendicular incidence, and according to equations [1.39] and [1.37] if the wave intersects the interface at an angle θ_i, with refraction of the transmitted wave according to equation [1.38]*

1.4.8. *Scattering and acoustic speckle*

When the variation of the acoustic impedance occurs for a structure that is on the order of the same size or smaller than the wavelength of the interrogating ultrasound pulse, the sound is not reflected but scattered. As the name implies, scattering

redirects part of the incident intensity in many directions. Since intensity is expressed in terms of the power per unit area, a scattering cross-section can be defined for any scattering object to conveniently express how much power will be scattered by the object for any given incident intensity. In other words, by calculating the product of the object's scattering cross-section and the incident intensity, the total power scattered by the object is found:

$$\text{scattered power} = \text{incident intensity} \times \text{scattering cross-section} \quad [1.40]$$

For a rigid spherical scatterer with a radius a that is much smaller than the ultrasound wavelength, the scattering cross-section increases as a function of frequency, f, (f^4) and also as a function of the scatterer's radius, a, (a^6). The scattering cross-section is also greater when there is a more marked difference between the compressibility and density of the scatterer and the surrounding medium. The scattered signals from blood are about 20 dB lower than those from tissue parenchyma.

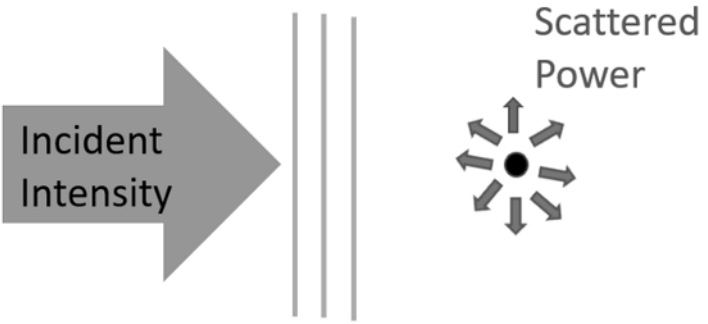

$$\sigma_{Total} = \frac{P_{Total\ scattered}}{I_{Incident}} \qquad \sigma_{B.S.} = \frac{P_{Backscattered}}{I_{Incident}}$$

Figure 1.12. *A structure much smaller than the acoustic wavelength scatters part of the incident intensity in many directions. The part of the power backscattered towards the transducer can be related to the incident intensity by the backscatter cross-section,* $\sigma_{B.S}$

Since the ultrasound probe is used in pulse-echo mode to detect scattering, the backscattered power that is returned for detection by the transducers in the probe is the only part of the scattered intensity that is of interest. This can be calculated based

on the part of the power returned within a limited solid angle oriented back towards the transducer probe. Thus, in general, it is the backscatter cross section describing this portion of the total scattered power that is of interest.

For a cellular-sized structure in the body, the backscatter cross section is very small (on the order of 10^{-18} cm^2), but since the ultrasound probe will receive power scattered from many such tiny scattering structures simultaneously, a detectable signal can be obtained. Because these scattering structures are arranged in a random fashion on a scale that is very small compared to the ultrasonic wavelength, the signals returned to the probe will interfere with each other. Whether the interference is positive or negative will depend on the random spatial organization of the scattering structures. This interference between echoes from the fluctuations of the acoustic impedance due to tiny structures in the tissue that are much smaller than the ultrasonic wavelength results in a grainy pattern on ultrasound images that is referred to as ultrasonic speckle. Experienced radiologists can perceive different speckle patterns and integrate this information into their diagnostic process. However, the speckle pattern also reduces the level of contrast between different types of media.

1.4.9. *Cavitation and the mechanical index*

The peak negative pressure used for ultrasonic imaging in tissue must be limited to avoid the risk of creating cavitation. In effect, if the negative pressure (rarefaction) created by the ultrasonic wave is too strong, pockets of gas can be created.

The mechanical index, MI, is defined as:

$$MI = \frac{derated\ peak\ rarefactional\ pressure\ (MPa)}{\sqrt{center\ frequency\ of\ the\ pulse\ (MHz)}} \quad [1.41]$$

To obtain the derated peak rarefactional pressure, in general, the pulse pressure is initially measured with a calibrated hydrophone placed at the desired distance from the transducer in a water path. The attenuation coefficient for the biological tissue to be imaged with the transducer is then applied to estimate the derated pressure. The FDA imposed limitation on the MI for diagnostic ultrasound is 1.9.

1.4.10. *Heating and the thermal index*

The heat absorbed by the medium must be limited during imaging. As the wave is attenuated, part of its energy is absorbed by the medium and this leads to heating.

Heating can become significant if the ultrasound waves have a high intensity or if the media interacting with the ultrasound are highly attenuating.

The thermal index, TI, is defined as:

$$TI = \frac{Power\ output\ (Watts)}{Power\ required\ to\ raise\ temperature\ by\ 1°C\ (Watts)} \quad [1.42]$$

The power required to raise the temperature by 1°C depends on the type of medium that is being insonified. For example, tissues that are well perfused with blood will require more power to induce heating than poorly vascularized tissues. Strongly absorbing materials such as bone will heat more readily.

A TI < 1 is considered to be safe for early fetal screening. The FDA limit for the spatial peak temporal average intensity is 720 mW/cm^2 during fetal imaging. Using a heating model, more precise estimates of the temperature rise can be obtained for different depths, types of tissues or exposure times.

1.4.11. *Radiation pressure*

Acoustic radiation pressure is produced when momentum from the acoustic wave is transferred to an absorbing or reflecting medium to create a displacement. This uniaxial force can be produced by focusing bursts of compressional ultrasound within a medium. Radiation pressure can be used, for example, to create push and release forces that act as sources for shear wave elastography techniques, as described in section 3.4.2.

1.5. Forming an image

1.5.1. *An array of signals that can be viewed in many ways*

Each ultrasonic pulse sent into the medium propagates deeper and deeper into the tissue. When it is reflected or scattered by inhomogeneities in the medium, echoes are created with a tiny fraction of the intensity of the interrogating ultrasound wave. These low-intensity echoes propagate back to the transducer, which sensitively detects the tiny vibrations and re-converts them into electrical signals which are then processed by the system.

A single scan line is referred to as an A-mode signal. The echoes returned to the probe are converted into relative amplitudes associated with a specific line of sight. The relative amplitude of this signal, related to the relative echogenicity of

structures encountered by the ultrasonic pulse, is recorded as a function of time. This fast time scale describes the propagation of the ultrasonic pulse to successive depths. Thus, the depth of each echogenic structure can be estimated by echo-ranging according to equation [1.1].

A single scan line can be presented as a function of time in M-mode to look along a single line of sight. The position of echoes on the M-mode will be displaced as objects move over time. Adjacent M-mode lines are separated in time on the scale of the pulse repetition interval, T_{PRI}.

For a B-mode image, scan lines from adjacent lines of sight are assembled to form an image within a plane where stronger echoes are displayed as brighter levels of gray. The time required to form such an image is known as the frame-rate.

When a sequence of images is acquired, signals acquired along a specific line of sight can be compared between consecutive image frames. The time between matched lines-of-sight from consecutive images is determined by the time required to acquire each image (the inverse of the number of frames per second, FPS).

1.5.2. *Diffraction and natural focusing*

Diffraction describes how the waves from a finite source spread out and interfere with each other. For a simple, continuous wave (CW) single-element transducer with finite dimensions, every point on the transducer's surface can be considered as a source of spherical wavelets according to the Huygens principle. These wavelets propagate outward, away from the source and interfere constructively and destructively when individual wavelets are strongly out of phase with each other. This interference is very strong when the wavelets are close to the source (in the near field or in the Fresnel zone) so that the pressure wave is very irregular in the near field. The diffraction of the source also leads to side lobes. A larger transducer element diameter or longer wavelengths will lead to reduced side lobes.

The near-field boundary is at the axial position of the last maximum in field pressure. This occurs at a position that is approximately equal to the square of the radius of the transducer element divided by the wavelength of the transmitted wave. At this "natural focus", there is constructive interference of the wavelets from the source. The transducer surface can be shaped to place the constructive interference at a desired point referred to as the focal point. Beyond the near-field boundary lies the far field or the Fraunhofer zone in which the approximately planar wavefront diverges and decreases steadily in intensity.

1.5.3. *Electronic focusing versus ultrafast plane waves*

Ultrasound arrays are made up of hundreds of transducer elements. Each individual PZT element has a width on the order of the ultrasound wavelength and is mechanically and electrically isolated so that each element can be activated with different time delays to steer or focus the array's beam. Since the intensity of the field is increased in the focal zone, the backscattered power (echoes) from structures in these zones is increased and objects near the focal zone can be detected with greater sensitivity. This method of conventional focused imaging applies selected delays for a sub-set of the array elements to focus the acoustic pulse along one line of sight within the imaged medium. Echoes returned from that line of sight are reconverted into electrical signals by the elements of the transducer and processed to form one collected scan line. If 256 adjacent scan lines are focused and collected to reconstruct an image of the medium, it is necessary to wait the time needed for 256 acoustic round trips from the transducer to the deepest point in the image and back to the transducer to obtain all the information needed to form the image. For focused ultrasound imaging, frame rates are typically on the order of 30–50 frames/s.

Plane-wave imaging does not apply time delays to focus the emitted beam on a specific zone of the image. All structures within the scan plane are more uniformly insonified, and echoes returned from all regions of the scan plane will be on the same basic footing in terms of echo intensity. Plane-wave imaging can provide much higher scanning rates because the entire plane is insonified with ultrasound in a single shot and then all the echoes from all regions of the imaged plane are collected. Echoes from multiple scattering structures can have the same pulse-echo propagation times. For example, echoes from a deep region along the direct line of sight for one of the elements of the transducer will be returned to that element at the same time as echoes from a more shallow zone at some angle off of the central axis. Thus, computer analysis must be applied to interpret the signals and form an image. This single-shot and off-line numerical reconstruction process is much faster than conventional focused ultrasound, but the contrast of the reconstructed image is much lower. Contrast can be recuperated, however, if several plane waves with slightly different angles of incidence are used to insonify the medium and then the final image reconstruction is based on this multi-angle plane-wave dataset. Use of multiple angles reduces the frame rate but, in general, only a few tens of angled plane waves are needed to recuperate image contrast upon reconstruction. Thus, the final frame rate is still much more rapid than for conventional focused ultrasound, which must form hundreds of focused scan lines to form an image. For plane-wave imaging, the fundamental limitation on the frame rate comes from the time required for one round trip from the transducer to the deepest zone in the image and then back again. This can be further divided by the number of plane-wave angles

acquired to improve contrast in the reconstructed image. For example, if the frame rate for a single-angle plane-wave acquisition is 18,000 frames/s, the frame rate for plane-wave image reconstruction using such plane-wave acquisitions along 40 slightly different angles would be 450 frames/s.

1.5.4. *Key technical innovations*

Data analysis is now faster and largely software-based thanks to GPU (Graphical Processing Unit) technology. Coupled with the recent development of open platform ultrasound systems, more flexible programming of new and ultrafast sequences is now possible with access to emission and receive data. Programmable and ultrafast ultrasound systems are the key behind shear wave elastography, functional ultrasound imaging of the rat brain and ultrafast ultrasensitive Doppler, discussed briefly in section 4.4.3.

Ultrasound is also becoming more portable. For example, CMUT probes consist of tiny membranes printed on an integrated circuit that provide an electro-mechanical connection with the membrane's movement. CMUTs can do lots of processing within the probe itself and be connected to an iPad or iPhone for mobile ultrasound. Three-dimensional imaging systems with a 2D transducer matrix are also becoming more prevalent. This is a key to reducing operator dependence due to image-plane choice from ultrasound evaluations.

1.5.5. *Time gain compensation*

Since attenuation leads to a relationship between the probe frequency and the accessible depth, and since this effect has an impact on the frequency content of the propagating wave, time gain compensation can be applied to amplify signals returning from deeper regions more strongly than signals returning from less deep regions. The gain at each depth can be adjusted by the operator.

1.5.6. *Contrast-to-noise ratio*

Objects with uniform composition will appear speckled on ultrasound images, and this makes the detection of irregularities more difficult. Clutter due to reverberations, sidelobes and other artifactual signal sources can lead to echoes that are out-of-place and therefore can mask the detection of structures of interest. These effects limit the contrast-to-noise ratio and can limit the sensitivity to detect small diameter or low contrast irregularities.

1.5.7. *Beam volume and spatial resolution*

The spatial resolution is defined based on the minimum separation between two different objects that allows them to be discriminated from each other. For an ultrasound array, this resolution is different for each of the three dimensions concerned by the image: the lateral dimension running parallel to the axis of the array, the axial dimension along the axis of ultrasound propagation and the elevational or out-of-plane dimension.

The lateral resolution is limited by the wavelength, λ, and the geometry of the transmitting elements in the array because the extent of the zone into which we can focus energy will determine how far apart objects must be along the lateral axis in order to be resolved:

$$Lateral\ Res. \approx \frac{1.22 \cdot \lambda \cdot Focal\ length}{Transmitting\ aperature\ diameter} \quad [1.43]$$

In depth, echoes received from two objects that are aligned along the axial direction must return to the transducer at times that are sufficiently separated to distinguish the signals scattered from each object. This is determined by the spatial pulse length, which is usually on the order of 1.5–2 wavelengths. The spatial pulse length, *SPL*, and the pulse duration, *PD*, are very simply related:

$$SPL = [\#\ cycles\ in\ pulse] \times \lambda = [\#\ cycles\ in\ pulse] \times \tau \times c = PD \times c \quad [1.44]$$

The axial resolution is given by:

$$Axial\ Res. = \frac{c \times PD}{2} = \frac{SPL}{2} \quad [1.45]$$

The elevational resolution is perpendicular to the image plane. For a linear array, this out-of-plane resolution is a function of the PZT element height and the characteristics of the fixed focal lens on the face of the transducer array.

1.5.8. *Pulse repetition frequency and frame rate*

The pulse repetition frequency, PRF (the fastest rate at which ultrasound pulses can be sent and received to interrogate a region), is the inverse of the time-to-echo from the deepest region of the image:

$$PRF = \frac{1}{T_{PRI}} = \frac{1}{TE_{Max\ depth}} = \frac{c}{[greatest\ distance\ of\ interest] \times 2} \quad [1.46]$$

For example, for 6 cm (or 60 mm), the $TE_{Max\ depth}$ is 80 microseconds and the PRF is 1/(80 μs) or 0.0125 pulses per μs (12.5 kHz or 12,500 pulses per second).

The time required to scan an entire image is only limited by the $TE_{Max\ depth}$ and the number of times such a round trip is necessary to form an image:

$$Time\ per\ image = [\#\ scan\ lines] \times TE_{Max\ depth} = \frac{\#\ scan\ lines}{PRF} \qquad [1.47]$$

If focusing along 256 scan lines is required to construct a single image, the time to acquire one image will be equal to the number of scan lines (the number of pulses we need to create and detect in pulse-echo mode) divided by the PRF. So, 256 divided by 12.5 pulses per millisecond, which is 20.48 milliseconds per image (0.02048 seconds per image). The number of image frames per second, FPS, that can be acquired is simply the inverse of the number of seconds needed to acquire each image

$$FPS = \frac{1}{Time\ per\ image\ [seconds]} \qquad [1.48]$$

In the example considered above where 20.48 milliseconds are required per image (0.02048 seconds per image), the FPS is approximately 48.8 frames per second. The FPS is directly proportional to the PRF and inversely proportional to the number of sequential transmit events required to scan the imaged region.

If a full image is scanned with a single pulse-echo event initiated by transmitting simultaneously with all the array elements at once using plane-wave imaging, the time per image is simply 1/PRF, or 80 μs per image (0.00008 seconds per image) for the example considered above, so that the FPS for such a plane-wave system would be 12,500 images per second. This series of examples show that focusing along 256 scan lines to image a 6 cm depth can provide about 49 frames per second, while plane-wave ultrasound can acquire data from the same zone at a rate of up to 12,500 frames per second. Plane-wave ultrasound provides an enormous time resolution advantage.

1.6. Imaging modes to further probe living systems

1.6.1. *Doppler*

If a source creates a sound wave while moving towards an observer, the observer will encounter the successive peaks and troughs of the waves more frequently due to the source's motion (see Figure 4.1), and the observer will perceive a higher

frequency than the frequency emitted by the source. The opposite is also true. If the source is moving away from the observer, the observer will detect a sound with a lower frequency than that emitted by the source. The Doppler shift is perceived when a rapidly moving vehicle emitting a sound (for example, a car honking) passes an observer.

For continuous wave Doppler, a transducer transmits an ultrasonic wave with a frequency of f_0 that propagates at a speed of c_0 towards moving red blood cells that then scatter echoes as they move. This scattered wave is detected by a confocally aligned receiver, as diagrammed in Figure 4.2. The moving red blood cells intersect the incident ultrasonic wave while they are moving, so that the frequency of the incident wave on the red blood cells is shifted due to the component of their velocity along the propagation axis of the incident wave, $v(cos\,\theta)$. Then, the red blood cells scatter echoes in all directions as they continue to move, so that the frequency detected by the receiver has been shifted a second time due to the component of the velocity of the source scattering waves that lies along the beam axis of the receiving transducer, $v(cos\,\emptyset)$. The overall Doppler frequency shift of the received signal, Δf_D, is linearly proportional to the blood flow velocity, v, as described in the CW Doppler equation:

$$\Delta f_D \approx \frac{v(cos\,\theta + cos\,\emptyset)}{c_0} f_0 \qquad [1.49]$$

To estimate the blood flow velocity from the Doppler frequency shift, the angles, θ and $\emptyset$, between the transmit and receive beams relative to the direction of the blood flow must be known (see Figure 4.2). The Doppler frequency shift detected from physiological blood flow using an ultrasound system operating at frequencies in the MHz range will fall within the audible range, at frequencies of a few kHz so that the information can be conveyed audibly. If the depth of the vessel allows the use of a higher transmit frequency, f_0, the intensity of backscatter from the rather weakly scattering red blood cells can be increased and, since the Doppler shift is proportional to f_0, a greater Doppler frequency shift can be obtained for a given blood flow velocity. The Doppler shift is also greater and subject to less error when the transducer beams and the direction of blood flow are well aligned (θ and ϕ are very small angles). CW Doppler is sensitive to all movements within the confocally aligned region of the two transducer beams, and a range of Doppler shifts corresponding to a range of velocities within the region of overlap between the two transducers will be obtained. It may be necessary to apply a high pass filter to exclude the detection of movement from strongly scattering but slowly moving tissue.

Pulsed Doppler systems allow the use of a single transducer in pulse-echo mode to estimate blood flow motion based on the time-of-flight shifts of echoes returned after consecutive pulsing events (see Figure 4.4). To construct the pulsed Doppler signal, the inter-pulse phase shift of echoes returned from a specific axial depth is evaluated based on the signal amplitude at that fixed axial depth sampled at the time of each successive pulse. The pulsed Doppler signal is sampled in time at an interval equal to the pulse repetition interval, T_{PRI}, that is referred to as slow time. The frequency spectrum of the pulsed Doppler signal is found from its discrete-time Fourier transform. Each frequency, f_D, in this spectrum can be related to a blood flow velocity, v, as described in the pulsed Doppler equation which very closely resembles the CW Doppler equation:

$$f_D = \frac{2v \cdot cos\,\theta}{c_0} f_0 \qquad [1.50]$$

As for CW Doppler, a range of frequency shifts are detected and the relative proportion of flow at different speeds is related to the relative intensity of the spectrum at each frequency. There are, however, some very important differences. First, the pulsed Doppler estimate can be more tightly localized to a time-gated zone within the beam's focal zone. Furthermore, aliasing can occur if the movement to detect is insufficiently sampled in time. To evaluate rapid blood flow, this effect can be overcome by increasing the pulse repetition frequency, PRF. Recall, however (see section 1.5.8), that the PRF is the inverse of the time-to-echo from the deepest region of the image so that increasing the PRF will decrease the explorable depth.

The smallest Doppler frequency (smallest blood flow) that can be detected with pulsed Doppler is limited by the bin size of the spectrum calculated from the Doppler signal:

$$f_{D\_Min} = \frac{PRF}{Number\ of\ samples\ in\ the\ pulsed\ Doppler\ signal} \qquad [1.51]$$

so that to detect very slow flow, it may be necessary to reduce the PRF or detect echoes from a greater number of pulse-echo sequences. Much more extensive information on Doppler-related techniques, their display and advances enabled by high-frame-rate systems is provided in Chapter 4, and its use in echocardiography is presented in Chapter 5.

1.6.2. *Shear wave propagation speed and elastic properties*

The longitudinal compressional waves used for ultrasonic imaging are presented in section 1.3.1. A second kind of wave, shear waves, can also propagate in an

elastic medium when a shearing force is applied. Shear waves do not propagate as readily in biological media as compressional waves, and their speed of propagation is much slower (~1–20 m/s) compared to compressional waves (~1,500 m/s). Since they propagate much more slowly than longitudinal compressional ultrasound, and since the propagation speed of these waves is related to the shear elastic modulus of the medium, it is possible to interrogate a medium with ultrafast, compressional pulses to track speckle decorrelation that occurs as a shear wave moves through a region. This can be used to assess the shear wave speed and thus to estimate medium elastic properties. Biological tissues are not perfectly elastic, but are rather viscoelastic. This means that there is a frequency-dependent delay in the strain response. This feature can be used to assess the viscosity of a medium. Shear wave propagation, the challenges of creating shear waves in biological media and their use for elasticity assessment are presented in Chapter 3.

1.6.3. *Ultrasound contrast imaging*

Ultrasound contrast imaging relies on the intravascular injection of exogenous microbubbles with a unique acoustic response (resonance, nonlinearity, destruction), which can be used to enhance the Doppler SNR, for tracer-perfusion modeling of the microvascular flow or for ultrasound localization microscopy. Microbubbles contain a gas and so, relative to the surrounding blood, they present a very strong acoustical impedance mismatch and scatter ultrasound very efficiently. Since they are micrometric in size, they remain within the vascular tree and are not spatially resolved on ultrasonic images. Once injected, microbubbles flow along with the red blood cells so they can be used as tracers of blood flow. After injection, the signal from the circulating bubbles is only visible for a few minutes because they are progressively taken up into the liver, and the gas that they contain is ultimately diffused through the lungs.

The acoustic impedance mismatch is not the only factor that favors the detectability of ultrasound contrast microbubbles. The radius and compressibility of microbubbles are also very important. When exposed to the pressure changes caused by ultrasound, these highly compressible microbubbles present resonant behavior and the bubble wall can oscillate nonlinearly about its equilibrium position. The resonance for microbubbles able to pass through the capillary bed happens to fall within the frequency range used in diagnostic ultrasound. When microbubbles oscillate in a nonlinear manner, they can be more sensitively detected relative to surrounding media due to the specific frequency content, amplitude or phase of their response. Thus, specific pulse-sequences can be used to highlight the nonlinear behavior of microbubbles. They can also be detected based on their acoustic

disruption. To evaluate microvascular flow, even though tiny vessels and microbubbles are too small to resolve, the time-dependent modification of nonlinear echoes received from contrast agent microbubbles moving with very slow speeds can be related to blood flow and relative blood concentration within a region of interest. Ultrasound contrast agents and the methods enabling their use to assess the microvascularization are presented in detail in Chapter 6.

1.6.4. *Super-resolution imaging*

Tracer-based contrast imaging provides highly useful information, but it would be nice to map out the vessels within organs such as the brain, kidney and tumors. Increased resolution cannot be obtained by increasing the ultrasound frequency because the attenuation at high frequencies strongly limits the penetration depth. Although it is not possible to spatially resolve an individual microbubble because the image resolution is limited by beam diffraction, it is possible to detect a single microbubble. This is the key premise of ultrasound localization microscopy or super-resolution imaging that is presented in much greater detail in Chapter 7. Since each contrast microbubble is much smaller than the wavelengths used to image them, by localizing the center of an individual microbubble source on an ultrasound image, the diffraction resolution limit can be defied to image fine vascular structure. By using ultrafast imaging, it is further possible to track individual microbubbles to obtain information about the flow rate and direction on a scale down to about 10 microns.

1.6.5. *Photoacoustic imaging*

Photoacoustic imaging is based on the fact that acoustic signals can be detected when optical absorbers undergo thermoexpansion. Thus, by illuminating zones within tissue using a laser pulse, acoustic signals can be detected to map out structures with different optical absorption characteristics. Depths of a few centimeters can be imaged using this approach. The spatial resolution of the image depends on the resolution of the ultrasonic detection. A very complete description of photoacoustic imaging and its applications is provided in Chapter 9.

1.7. References

Chen, C. and Pertijs, M.A.P. (2021). Integrated transceivers for emerging medical ultrasound imaging devices: A review. *IEEE Open Journal of the Solid-State Circuits Society*, 104–114. doi: 10.1109/OJSSCS.2021.3115398.

Christensen-Jeffries, K., Couture, O., Dayton, P.A., Eldar, Y.C., Hynynen, K., Kiessling, F., O'Reilly, M., Pinton, G.F., Schmitz, G., Tang, M.X. et al. (2020). Super-resolution ultrasound imaging. *Ultrasound in Medicine & Biology*, 46, 865–891.

Cobbold, R.S.C. (2006). *Foundations of Biomedical Ultrasound*. Oxford University Press, Oxford.

Evans, D.H. and McDicken, W.N. (2000). *Doppler Ultrasound: Physics, Instrumentation and Signal Processing*, 2nd edition. Wiley, Chichester.

Hill, C.R., Bamber, G.R., ter Haar, G.R. (eds) (2004). *Physical Principles of Medical Ultrasonics*, 2nd edition. Wiley, Chichester.

Leighton, T. (1997). *The Acoustic Bubble*, 1st edition. Academic Press, London.

Lindner, J.R. (2004). Microbubbles in medical imaging: Current applications and future directions. *Nature Reviews Drug Discovery*, 6, 527–532. doi: 10.1038/nrd1417.

Montaldo, G., Tanter, M., Bercoff, J., Benech, N., Fink, M. (2009). Coherent plane-wave compounding for very high frame rate ultrasonography and transient elastography. *IEEE Transactions on Ultrasonics, Ferroelectrics and Frequency Control*, 56, 489–506. doi: 10.1109/TUFFC.2009.1067.

Szabo, T.L. (2013). *Diagnositic Ultrasound Imaging: Inside Out.* Academic Press, New York.

Tanter, M. and Fink, M. (2014). Ultrafast imaging in biomedical ultrasound. *IEEE Transactions on Ultrasonics, Ferroelectrics, and Frequency Control*, 61, 102–119. doi: 10.1109/TUFFC.2014.2882.